Interaction of CO$_2$ laser-modified nylon with osteoblast cells in relation to wettability.

D. G. Waugh[1], J. Lawrence[1], D. J. Morgan[2] and C. L. Thomas[3]

[1]Wolfson School of Mechanical and Manufacturing Engineering, Loughborough University, Leicestershire, LE11 3TU, UK
[2]Cardiff Catalysis Institute, School of Chemistry, Cardiff University, Cardiff, CF10 3AT, UK
[3]Healthcare Engineering, Loughborough University, Leicestershire, LE11 3TU, UK

Corresponding Author:

Mr. David G. Waugh
Wolfson School of Mechanical and Manufacturing Engineering
Loughborough University
Loughborough, UK
LE11 3TU

Tel: 01509 267614
Fax: 01509 227648
Email: D.G.Waugh@lboro.ac.uk

1

1 - Abstract

It has been amply demonstrated previously that CO_2 lasers hold the ability to surface modify various polymers. In addition, it has been observed that these surface enhancements can augment the biomimetic nature of the laser irradiated materials. This research has employed a CO_2 laser marker to produce trench and hatch topographical patterns with peak heights of around 1 μm on the surface of nylon 6,6. The patterns generated have been analysed using white light interferometery, optical microscopy and X-ray photoelectron spectroscopy was employed to determine the surface oxygen content. Contact angle measurements were used to characterize each sample in terms of wettability. Generally, it was seen that as a result of laser processing the contact angle, surface roughness and surface oxygen content increased whilst the apparent polar and total surface energies decreased. The increase in contact angle and reduction in surface energy components was found to be on account of a mixed intermediate state wetting regime owing to the change in roughness due to the induced topographical patterns. To determine the biomimetic nature of the modified and as-received control samples each one was seeded with 2×10^4 cells/ml normal human osteoblast cells and observed after periods of 24 hours and 4 days using optical microscopy and SEM to determine mean cell cover densities and variations in cell morphology. In addition a haeymocytometer was used to show that the cell count for the laser patterned samples had increased by up to a factor of 1.5 compared to the as-received control sample after 4 days of incubation. Significantly, it was determined that all laser-induced patterns gave rise to better cell response in comparison to the as-received control sample studied due to increased preferential cell growth on those surfaces with increased surface roughness.

Keywords: CO_2 laser, nylon 6,6, wettability, osteoblast cells, bioactivity

2 – Introduction

It is seen that nylon can be utilized within the biomaterial industry as sutures [1], vascular grafts [2] and other hard tissue implants [3]. By extrapolating from past and current research it is imperative that any biomaterial should be optimized in order for that material to function appropriately and efficiently within the desired biological environment. In numerous instances it is seen that the bulk properties of a biomaterial are decided upon such that the surface properties are compromised [4,5]. In particular, this is seen throughout the use of polymeric biomaterials as they offer excellent bulk properties for biological applications; however, the surface properties they possess do not lend themselves to high performance in regards to biomimetics [6]. On account of this, it is necessary to vary the surface properties of the material without hindering the bulk properties in order to enhance the wettability and bioactivity. In terms of bioactivity a biomaterial can be surface modified both topographically and chemically in order to manipulate the way in which the cells react. That is the signaling of the cells

could be optimized in order for the filopodia to assess the extracellular matrix (ECM) and substrate so that the most possible integrin receptors could be localized around the suitable binding site to improve upon adhesion characteristics [7]. This is of great importance to those cells such as osteoblast cells that are highly dependant on ECM anchorage and as a direct result necessitates adhesion with the biomaterial prior to the initialization of normal cell function [8]. Integrin receptors are crucial to the way in which a biomaterial is accepted into the biological environment insofar as cellular interactions takes place through the receptors creating focal adhesions. These focal adhesions are also important as they produce a high density of adhesion transmembrance receptors in areas of cellular adhesion to the biomaterial owed to the fact that they are closely associated with the actin cytoskeleton and other factors which regulate the signaling that takes place as the cell functions [9].

One of the most interesting subject areas in biomaterials surface science is that of wettability, with many workers endeavoring to determine the complex links between surface wetting and bioactivity [10]. Numerous theories have been expressed in order to explain this phenomenon in which two basic regimes have arisen. The first takes the biomimetic properties and attempts to correlate it with the surface energy whilst the second involves water solvent properties near the surface in which a correlation between the contact angle and bioactivity is strived for. However, in both cases a fundamental factor dominates in which the surface energy/wetting is generally related somewhat to the biological response [11]. Various approaches have been undertaken as to ascertain quantitative reasoning to bioactivity such as Van Oss *et al.* [12] by using the 'equation of state' approach to calculate interfacial tensions from previously measured contact angles in order to attempt and predict cell adhesion. Such approaches have been found to fall short for achieving a quantitative theory regarding the bioactivity of a material. Through the available literature it can be seen that extensive research is now being carried out regarding this in the attempt to link wettability and bioactivity of materials [13,14]. Once a quantitative link has been forged between these two parameters one can extrapolate that this will give those throughout the biotechnological industry a means to produce materials which have the ability to either enhance or even hinder the biomimetic nature; for instance, materials produced with surfaces that hinder the growth of bacteria could be widely used throughout the food packaging industry. On the other hand, enhanced biomimetics could be utilized for numerous applications such as biological implants and BioMEMs applications [15].

Numerous techniques have been developed that have the ability to modify the surfaces of different materials [16]. Some of these methods are radiation grafting [17], plasma surface modification [18,19] and using various coatings [20]. Another method which has the ability to produce surface modifications is that of laser treatment [21,22] and offers a number of benefits such as accurate, precise, non-contact and clean processing. One other major advantage that lasers offer over other competing techniques is that they can produce micro and nano scale topographical and surface chemical variations with negligible affect to the bulk properties of the material. Also, it should be

noted that as most laser systems are now automated this technique holds the ability to be used for large area processing. Being able to produce these topographical and surface chemical variations can be seen to be of great advantage when applying laser surface modification to fields such as biomimetics especially as previous work has shown a very high dependence of micro and nano scale topography and surface chemistry on the cell-material interaction [7-9,15,16,22,23].

On account of the numerous advantages laser materials processing has to offer for laser surface treatment it is necessary that considerable research is undertaken to ascertain how this technique can be employed in such fields as biotechnology. Such research will lead to the ability of assessing the plausibility and reliability for using lasers to produce surface modifications to aid in the enhancement of the biomimetic nature of biomaterials. On account of the required significant research in this field the first ever initial study into how CO_2 laser generated surface patterns influence both the wettability characteristics of nylon 6,6 and normal human osteoblast cell response, when studied *in vitro*, has been carried out. This investigation has taken place in order to study how the biomimetic nature of laser surface patterned nylon 6,6 can be affected by surface properties such as characteristic recently advancing contact angle, surface roughness, surface oxygen content and the surface energy.

3 – Experimental Techniques

3.1 – Laser Irradiation Procedure

The nylon 6,6 was sourced in 100×100 mm^2 sheets with a thickness of 5 mm (Goodfellow Cambridge, Ltd). To obtain a conveniently sized sample for experimentation the as-received nylon sheet was cut into 30 mm diameter discs using a 1 kW continuous wave (cw) CO_2 laser (Everlase S48; Coherent, Ltd). No discernible heat affected zone (HAZ) was observed under optical microscopic examination.

In order to generate the required marking pattern with the 10.6 μm Synrad cw 10W CO_2 laser system Synrad Winmark software version 2.1.0, build 3468 was used. In addition, the software was capable of using images saved as .dxf files which can be produced by using CAD programs such as, in this case, Licom AutoCaM. The nylon 6,6 samples where placed into the laser system onto a stage in which they where held in place using a bracket with a 30.5 mm diameter hole cut into the centre of the bracket. The surface of the sample was set to be 250 mm away from the output facet of the laser system to obtain focus and the system utilized a galvanometer scanner to scan the 95 μm spot size beam directly across the stationary target material. It should be noted that the target material and laser system was held in a laser safety cabinet in which the ambient gas was air and an extraction system was used to remove any fumes produced during laser processing.

20 samples were irradiated altogether to produce 4 identical 6-well plates with each corresponding well having the same pattern. These were named plates 1A, 1, 2 and 3. There were four patterns induced onto the surfaces of the nylon 6,6 samples which were trenches with 50 μm spacing (A3), hatch with 50 μm spacing (B1), trenches with 100 μm spacing (B2) and hatch with 100 μm spacing (B3). In addition, an as-received control sample was used (A1). For each of the irradiated patterns the laser power was set to 70% (7 W) operating at 600 mms^{-1}.

3.2 – Topography, Wettability Characteristics and Surface Chemistry Analysis

After the laser irradiation of the nylon 6,6 samples plate 1A was analysed using a number of techniques. An optical microscope (Flash 200 Smartscope; OGP, Ltd) was used to obtain optical micrographs of the samples. The surface profiles were determined using a white light interferometer (WLI) (NewView 500; Zygo, Ltd) with MetroPro and TalyMap Gold Software. The Zygo WLI was setup using a ×10 Mirau lens with a zoom of ×0.5 and working distance of 7.6 mm. This system also allowed Sa and Ra roughness parameters to be determined for each sample.

In accordance with the procedure detailed by Rance [24] the samples were ultrasonically cleaned in isoproponal (Fisher Scientific Ltd., UK) for 3 minutes at room temperature before using a sessile drop device to determine various wettability characteristics. This was to allow for a relatively clean surface prior to any contact angle measurements being taken. To ensure that the sample surfaces were dry a specimen dryer (Metaserv, UK) was utilized to blow ambient air across the samples. A sessile drop device (OCA20; Dataphysics Instruments, GmbH) was used with relevant software (SCA20; Dataphysics Intrsuments, GmbH) to allow the recent advancing and receding contact angles for triply distilled water and the recent advancing angle for diodomethane to be determined for each sample. From the measured advancing and receding contact angles the hysteresis for the system was established. Thereafter the advancing contact angles for the two liquids were used by the software to draw an Owens, Wendt, Rabel and Kaeble (OWRK) plot to determine the surface energy of the samples. For the two reference liquids the SCA20 software used the Ström et al. technique to calculate the surface energy of the material. It should be noted here that ten contact angles, using two droplets, in each instance was recorded to achieve a mean contact angle for each liquid and surface.

Selected samples were analysed using x-ray photoelectron spectroscopy (XPS) analysis. This allowed any surface modifications in terms of surface oxygen content due to the laser irradiation to be revealed. These samples were selected in terms of contact angle; the as-received reference sample, laser patterned sample with the lowest contact angle and the laser surface patterned sample with the highest contact angle was used. XPS measurements were performed on a Kratos Axis Ultra DLD photoelectron spectrometer employing monochromatic aluminium k-alpha radiation source, operating at 120W power and an associated photon energy of 1486.6 eV. To test the reproducability of the

surface, two sections of each sample were analysed; the analysis area on each sample was 700x300 microns. The spectrometer was run in its Hybrid mode and spectra were acquired at pass energies of 20 eV (for the high resolution scans) and 160 eV for the survey scans. All data was analysed through CasaXPS (v2.3.14) analysis software (ref: http://www.casaxps.com) using sensitivity factors supplied by the instrument manufacturer.

3.3 – *In Vitro* Experimentation

Prior to any biological testing being carried out the samples were autoclaved (D-Series Bench-Top Autoclave; Systec, GmbH) to ensure that all samples were sterilized. For all biological work undertaken, unless stated, a biological safety cabinet (BSC) (Microflow Class II ABS Cabinet; BioQuell UK, Ltd) was used to create a safe working environment and to provide a clean, sterile environment to manipulate the cells used.

Normal human osteoblast cells (Clonetics CC-2538; Lonza, Inc.) were initially cultured in a T75 (75ml) flask by suspending the cells in 19 ml culture medium comprising of 90% eagle minimum essential medium (Sigma-Aldrich, UK) and 10% foetal bovine serum (FBS) (Sigma-Aldrich, UK). The flask was then placed in an incubator and left for 24 hours. After 24 hours the cells were assessed and the spent media was aspirated before dispensing 15 ml of fresh media and returning the flask to the incubator for 3 days.

The period of 3 days allowed the cells to become confluent in the flask providing enough cells for seeding onto the samples. The cells were detached from the flask using 5 ml Trypisn-EDTA (Sigma-Aldrich, UK) whilst placed in the incubator for seven minutes. Once all cells had become detached 10ml culture medium was added to neutralize the Trypsin. In order to aspirate the supernatant the cell culture was centrifuged (U-320R; Boeco, GmbH) for five minutes at 200 g. To ensure the cells were ready for seeding they were resuspended in 10 ml of culture medium and dispensed between the eighteen samples in the 6-well plates. This equated to 0.55 ml (2×10^4 cells/ml) for each sample. The well plates were placed in the incubator were plate 1 was removed after 24 hours and plates 2 and 3 after 4 days. Plates 1 and 2 were prepared for the SEM as will be discussed later and plate 3 was prepared for counting using an improved neubauer haemocytometer (Fisher Scientific, UK) by mixing 10 μl of each cell suspension with 10 μl of trypan-blue (Sigma-Aldrich, UK).

3.4 – SEM and Optical Microscopy Analysis of *In Vitro* Samples

In order to view the attached cells using SEM it was necessary to undertake a procedure to produce a sample that was dehydrated ready for Au coating. The samples were initially rinsed with phosphate-

buffered saline (PBS) (Sigma-Aldrich, UK) to remove any unattached cells and then adherent cells were fixed using 1.2% glutaraldehyde in water (Sigma-Aldrich, UK) at room temperature for 1 hour within the BSC. After an hour the glutaraldehyde solution was removed and the fixed cells were washed with PBS prior to carrying out a graded series of ethanol/distilled water mixtures of 50/50, 80/20, 90/10, 95/5, 98/2 and 100/0. Each sample was left in these mixtures for 10 minutes to ensure dehydration. Once this procedure was carried out the samples were mounted and sputter coated with Au so that SEM images could be obtained. In addition to SEM images, optical micrographs were obtained using an optical microscope (Optiphot; Nikon, UK) with a 5× Nikon objective lens, with images being captured using a microscope camera (WV-CL300; Panasonic, UK) along with DT Acquire Version 3.3.0 computer software (Data Translation Inc., USA). In order to produce the best images possible each image was manipulated in terms of brightness, contrast and gamma by using ImagePro Version 5.0.0.39 for Windows XP/Professional software (Media Cybernetics Inc., USA).

3.5 – Statistical Analysis

All statistical analysis was carried out using SPSS 16.0.2 for Windows software (SPSS Inc., USA) in order to analyse the data obtained using one-way ANOVA to obtain F-ratios and significance levels (p). In addition to ANOVA analysis post hoc multiple comparison tests in the form of Scheffe's range tests where performed in order to determine statistic significance between groups in which results are reported at a mean difference significance level of $p < 0.05$.

<div align="center">

4 – Results and Discussion

</div>

4.1 – Effect of Laser Irradiation on Topography

It has already been confirmed from previous work that the process in which the infra-red laser light couples into the nylon 6,6 is that of a thermolytical nature [25] rather than direct bond disassociation which occurs with UV lasers. That is, the irradiated surface becomes molten due to a rapid temperature rise which leads to a protrusion away from the surface as a direct result of flow within the molten material along with rapid resolidification as the beam moves away from that area. By utilizing the constant laser parameters of 7 W and a traverse speed of 600 mms^{-1} various patterns were induced onto the surface of the nylon 6,6. The continuous axonometric images for these patterns are shown in Figure 1.

It can be seen from Figure 1 that qualitatively the laser irradiated nylon 6,6 samples were considerably rougher in comparison to the as-received reference control sample. Further confirmation of this qualitative result was obtained by taking a profile extraction of each sample (see Figure 2). From

Figures 1(d) and (e) it was possible to ascertain that the resulting surface pattern was more defined in one axis of the hatch in comparison to the other. This is a resultant of the way in which the CO_2 laser marker scanned the input image onto the target sample.

The profile extractions for each of the samples shown in Figure 2 provides confirmation that the laser processing of the nylon 6,6 gave rise to a considerable variation in the surface topography. That is, the roughness had increased and slight periodicity in the laser patterned samples can be seen in contrast to the as-received reference control sample. In comparison to the as-received reference control sample, which had peak heights of the order of 0.1 to 0.2 μm, the peak heights for all of the laser treated samples were around 1 μm. It was also observed that the least periodicity arose from those samples which had patterns with 50 μm spacings . This can be seen to be of some importance as the laser spot size at the surface of the target samples was 95 μm consequently allowing the scans for the trenches and hatch patterns to overlap and ultimately eliminate the natural periodicity of the original scanned pattern. However, the scan overlap occurring did ensure that the whole of the surface of the target sample was irradiated and modified in comparison to the non-irradiated reference sample. For the laser surface modified samples (see Figures 2(b-g)) peak heights of approximately 1 μm was achieved.

4.2 – Effect of Laser Irradiation on the Wettability Characteristics

As already stated in the available literature, the surface properties of a material have a major influence on the way in which a liquid will react at the interface between the liquid and material surface. As such, the surface roughness parameters (Sa and Ra), contact angle for triply distilled water and surface energy parameters were determined for each sample and are given in Table 1.

The results given in Table 1 show that the laser surface treatment has given rise to sufficiently increased surface roughness in comparison to the as-received reference control sample (A1) with the largest Sa being 0.636 for the 50 μm trenches pattern (A3) and the largest Ra being 0.185 μm for the 100 μm trenches pattern (B2). It was also determined that the apparent polar component, γ^P, and total surface energy, γ^T, was seen to decrease for all laser treated samples compared to that of the as-received reference control sample. As a result of the reduction in apparent γ^P and the increase in surface roughness the recently advancing contact angle was seen to increase. As a direct result of this the resulting characteristic contact angle for the rougher samples increases; for instance, the 50 μm trench pattern (A3), with the maximum Sa of 0.636 μm and lowest γ^P of 12.24 mJm^{-2} gives the largest contact angle of 66.0°. Current theory states that for a flat hydrophilic surface an increase in roughness ought to result in the contact angle effectively decreasing [26]; however, as one can see from Table 1 this is not the case in this work for the hydrophilic nylon with contact angles with the

reference contact angle being 56.4° (A1). This can be explained by the likely existence of a mixed Cassie-Baxter/Wenzel state wetting regime, in which both Wenzel and Cassie-Baxter regimes are present over the solid-liquid interface [27-30]. That is the surface roughness along with the induced pattern yields a water droplet which is held in an intermediate state such that both wetting regimes coexist. This mixed wetting regime arising can also account for the observed reduction in apparent γ^P and increase in contact angle owed to the laser induced topographical pattern on the hydrophilic nylon 6,6 samples. Another factor which can be taken from Table 1 is that the hatch patterns (B1 and B3) gave rise to smoother surfaces in comparison to the trench patterns (A3 and B2). The reasoning behind this result is believed to be on account of the beam overlapping the same irradiated area numerous times during laser processing. This allowed the material to remelt, causing the resolidified material to become smoother as the sample surface cools. It should be noted here that the laser irradiated surfaces have higher errors for the contact angle measurement owing to the fact that surface topography would have affected how the liquid formed an equilibrium state on the material surface. To analyse the extent of the polar component/surface energy and surface roughness being a driving force on the contact angles, graphs of contact angle as a function of polar component/surface energy (see Figure 3) and Sa/Ra (see Figure 4) were drawn.

One can see from Figure 3 that the contact angle appears to have good correlation in conjunction to the two apparent surface energy components such that the recently advancing contact angle is a decreasing function of the apparent γ^P and γ^T. This coincides with current theory which states that the contact angle will decrease upon an apparent increase of the surface energy components that have been graphed in Figure 3 [4]. From this result one can extrapolate that the resulting contact angle for the laser surface treated nylon 6,6 is highly dependant on the apparent γ^T and γ^P and by knowing how laser treatment affects the surface energy of a polymeric material this could allow for a pre-determined contact angle to be achieved. In a similar manner, a graph of contact angle against the surface roughness parameters Sa and Ra was drawn, as seen in Figure 4, to ascertain if any correlation could be highlighted.

Due to the surface topography having a large effect on the wetting regime taking place it was necessary to analyse how the recently advancing contact angle varied over the different induced surface roughness values. Figure 4 shows that there is a significant difference between how the surface roughness parameters, Ra and Sa, relate to the recently advancing contact angle for triply distilled water incident on the laser surface treated nylon 6,6 samples. The data given in Figure 4 allows one to see that the roughness parameter Ra has a Gaussian fit with the contact angle measured giving a peak contact angle of around 65° to be obtained with an Ra value of around 0.1 μm. In contrast the Sa parameter gives a considerably different correlation such that contact angle remains constant around 56° for Sa values up to 0.3 μm at which point the angle begins to increase until it

finally plateaus from Sa values of 0.4 μm and more with contact angles of approximately 65°. This shows that there could be some dependence on the two surface roughness parameters in determining the contact angle; however, the resulting correlation does not appear to be as strong as shown with the surface energy components as seen in Figure 3. Another factor that should be considered in this instance is that the data given in Figure 4 does not necessarily coincide with current theory which states that for a hydrophilic material an increase in roughness should reduce the contact angle making the material more hydrophilic [4]. For both Ra and Sa parameters the contact angle increases from the initial contact angle obtained with the non-irradiated reference sample which, as stated previously, is attributed to the mixed state wetting regime taking place due to the topography of the laser surface treated samples. Having said that, it was observed using Figure 4 that the contact angle did decrease for larger Ra values arising from the laser patterned samples which does coincide with current theory which states that, under certain conditions, the contact angle is a decreasing function of surface roughness [31]. Nevertheless, it may still be possible to estimate the contact angle to be achieved by using the correlations that have been identified throughout this research. Following on from this, with the aid of being able to estimate the contact angle this could feasibly help to produce surfaces that give rise to enhanced cell adhesion and proliferation if the optimized contact angle or contact angle range was known for the cell type that would be coming into contact with that specific material.

In addition to surface energy and surface roughness the surface oxygen content of a material may have an affect on the resulting contact angle and following on from this the surface oxygen content for selected samples were chosen; these samples were the as-received reference control sample (A1), 100 μm trenches (B3) and 50 μm trenches (B1). These samples were chosen as they were the limits in terms of the recently advancing contact angles measured. On account of this the data given in Table 2 indicates that the surface oxygen content may not be one of the main factors that gives rise to the apparent increase in advancing contact angle as a rise in oxygen content should bring about a reduction in the contact angle as stated by Hao and Lawrence [5]. The slight rise in oxygen content can be attributed to oxidation of the nylon 6,6 surface during laser surface treatment as the experiments were carried out in ambient air. From the results shown in both Tables 1 and 2 the evident rise in contact angle can predominantly be a result of the reduction in the apparent γ^P on account of the mixed state wetting regime taking place owed to the surface topography. With this in mind it can be seen that the surface topography in terms of roughness and pattern can have a large effect on the extent of which wetting regime occurs and directly effects the value of the apparent γ^P and γ^T. Therefore, the polar component along with the surface roughness/topography can be seen to be the main driving force to defining the characteristic contact angle as they both are closely linked to one another in this instance.

4.3 – Effect of Laser Irradiation on Osteoblast Cell Bioactivity

4.3.1 – 24 Hours After Seeding

It has been seen that the laser material interaction has given rise to a sufficient modification in terms of numerous surface properties and as such it can be noted that this could have a large impact upon how the osteoblast cells react to the nylon 6,6 samples. Figure 5 shows the optical micrographs for the 6 Au coated samples 24 hours after cell seeding.

It can be seen in Figure 5 that for all samples the osteoblast cells have to some extent adhered to the differing surfaces. That is, the cells have firstly attached, adhered and have begun to spread across the surfaces. The extent to which this phenomenon has taken place appears to be dependant on the laser processing owed to the larger areas of cell coverage after 24 hours of incubation time. For the trench and hatch patterns the cells have somewhat proliferated resulting in the larger cover densities with the largest cell cover density being 37% for the 100 μm trench pattern which was considerably larger in comparison to the as-received reference control sample which gave rise to a mean cover density of 17%. It should also be noted here that from the micrographs shown in Figure 5 the laser treated samples do not appear to give rise to directionality in terms of cell growth and proliferation. In fact the cells seem to be growing in random directions in conjunction with the laser induced patterns. Additionally, in terms of morphology of the cells the micrographs in Figure 5 show that most of the samples gave rise to bipolar shapes, apart from the 100 μm trench pattern which was at a more advanced stage of the cell growth process. This could indicate that the growth process on the nylon 6,6 samples begins with a bipolar morphology and progresses to a more radial morphology as the incubated time progresses. To confirm what had been observed in the micrographs shown in Figure 5 the samples where analysed using SEM. The SEM images of each sample are shown in Figure 6.

The SEM images obtained in Figure 6 allowed one to confirm that the osteoblast cells were already at an advanced stage in terms of cell growth on the nylon 6,6 samples. This is owing to the cells beginning to spread over the sample surfaces. Also, both the micrographs and SEM images show that for all samples a number of cells had spread completely, forming numerous filopodias. In contrast to the micrographs in Figure 5, Figures 6(b) and (c) indicate that there may possibly be some directionality to the cell growth which is dependant on the surface topography; however, this is not conclusive and the non-directionality may well be a result of the relatively shallow peak heights forming the patterns which was determined in the profile extractions (see Figure 2) during the topography analysis. From Figures 5 and 6 it can be seen that the morphologies of the cells on each of the different samples are similar to one another which could indicate that the cells reacted in the same manner for each sample. However, it could have also potentially taken more than 24 hours to affect

the morphology of the cells and was considered when analysing the samples after the 4 day incubation period which will be discussed later. In addition, the SEM images shown in Figure 6 show that in some cases a bipolar morphology arises; however, the radial nature of the cell growth becomes more apparent on each of the samples when comparing the images in Figure 6 to those in Figure 5. This result also is an indicator to the fact that the cells in this instance do not have directionality owed to the laser-induced surface pattern.

In order to quantify how the osteoblast cells reacted to the different surface topographies the cell cover density was measured for each of the samples. A histogram showing the cover densities can be seen in Figure 7. In order to determine a mean value for the cover density four values were obtained from micrograph and SEM images.

The histogram given in Figure 7 shows that the mean cover density after 24 hours was larger for all laser irradiated samples in comparison with the as-received reference control sample. The largest mean cover density of 38% was achieved with the 100 μm trenches pattern, whilst the lowest was 17% for the as-received reference control sample. The 50 and 100 μm hatch patterned samples gave the lowest cover densities of 23 and 34%, respectively in comparison to the other laser patterned surfaces and can be owed to the roughness of these samples being less than the trench patterned samples. As a direct result of the mean cover density results shown in Figure 7 one can deduce that the laser surface modification implemented gave rise to an increase in proliferation, speeding up the cell growth process as a result of allowing the material to become more biomimetic by changing the surface characteristics.

4.3.2 – 4 Days After Seeding

With the 24 hour experiments showing that the cells had attached and begun to spread it was necessary to carry out analysis on the nylon 6,6 samples which had been seeded and incubated for 4 days to ensure that the cells where still adhered to the samples and that the spreading was still taking place. Figure 8 shows the optical micrographs obtained for each of the samples.

As one can see from Figure 8, after 4 days of incubation the cells were at an advanced stage of growth in comparison to the samples that had been incubated for 24 hours. This is due to the fact that all of the images in Figure 8 show that the cells have covered almost all of the surfaces of each sample with the least covered being the as-received reference control sample. This coincides with what was observed previously with the 24 hour incubated samples as the as-received reference control sample gave the least cover density in both instances. In addition it was also realized that the morphology of the osteoblast cells were very different when comparing each sample which had been left incubated

for 4 days. That is, the as-received reference control sample (see Figure 8(a)) produced a spindle-like radial morphology, the 50 μm trench/hatch (see Figures 8(b) and (d)) and 100 μm trench/hatch (see Figures 8(c) and (e)) gave rise to a clumped radial morphology but to varying extents on each of the different surfaces. This could be of a direct result of differing topographies between the different patterned samples as stated by Liang and Lawrence [5]. It should also be noted that similar to the 24 hour seeded samples the 4 day seeded samples did not appear to show any directionality in terms of growth and proliferation; however, for the 4 day seeded samples this may be due to the fact that every sample was tending towards 100% cover density. Again, for confirmation of what was observed with the micrographs shown in Figure 8 SEM images were taken, as can be seen in Figure 9.

From Figure 9 it is evident that the cells had rapidly begun to proliferate over the 4 day incubation period such that for all of the samples the cover density was tending towards maximum 100% cover density. The SEM images also showed that the cell growth was faster for the laser-induced trench and hatch patterns (see Figures 9(b, c, d, e)) in comparison to the as-received reference control sample. Upon closer inspection using the SEM as can be seen with the images in Figure 10, confirmation of the morphologies was carried out. From these images it was found that the as-received reference control sample (see Figure 9(a)) gave rise to a more coral-like morphology rather than spindle-like which was first thought with the micrographs shown in Figure 8. The 50 μm trench patterned sample (see Figure 9(b)) shows that the cell morphology was more clumped, spindle-like and was growing in a radial nature. The 100 μm trench patterned sample (see Figure 9(c)) was seen to produce a clumped radial cell morphology. Whereas the two hatch patterns (see Figures 9(d) and (e)) confirmed that the cell morphologies where clumped radial with the 50 μm trench pattern (see Figure 9(d)) appearing to be more coral-like.

The results in Figure 10 show that, on average, for each sample the cover density was approximately tending towards 100% thus allowing for no statistical significance to be obtained from the plotted data. This also implies that the seeded osteoblast cells over 4 days had covered all the surfaces of each sample regardless of how the surface was treated. Having said that, it should be noted that for the 100 μm hatch patterned sample each image used to calculate the cover density gave 100% covered resulting in the error being 0, as shown in Figure 10. There could therefore be some slight correlation between how the nylon 6,6 was treated prior to seeding and how the osteoblast cells react to the samples *in vitro*, although in reality no discernable relationship could be deduced from the data shown in Figure 10. As a result of the equivalent cover densities a cell count was also taken after the fourth day of incubation which can also be used to analyse how the cells react to the different patterned samples.

A graph of cell density count as a function of pattern can be seen in Figure 11 which indicates that there was a higher cell count after 4 days incubation for the trench and hatch patterns in comparison with the as-received reference control sample. This further suggests that the surface pattern/roughness had a significant effect on the cell response in terms of cell cover density and growth. Also, as evidenced by the different cell morphologies (see Figures 5, 6, 8 and 9), surface roughness does have a large influence on cell signaling in accordance with Nebe [32]. But, no discernible correlation between the cell density count and surface characteristics such as roughness and surface energy parameters could be determined in this instance, which could suggest that other factors might be in play such as surface charge or even suggest that a number of different parameters are contributing to the osteoblast cell response. Although it has been seen throughout this study that surfaces which have been almost fully treated with the CO_2 laser beam give rise to improved cell adhesion, proliferation and as such promotes a better interface for mitosis to take place.

5 – Conclusions

Through this study it has been determined that following CO_2 laser processing of nylon 6,6 the surface characteristics can be modified in order to have influence over the recently advancing contact angle. From analysing the laser induced patterned surfaces it was found that the surface energy and polar component had decreased by up to 7 mJm^{-2} and the surface roughness had considerably increased. It was found that the apparent polar component and total surface energy for the samples studied were both a decreasing function of the characteristic advancing contact angle, which correlates with current theory; however, current theory states that the contact angle for a hydrophilic surface should decrease upon increasing surface roughness which has not been seen throughout this experimentation. This can be attributed to an intermediate mixed Cassie-Baxter/Wenzel regime, in which both Wenzel and Cassie-Baxter regimes arise at the solid-liquid interface as a result of the formation of the water droplet on the various laser modified surface topographies. Another factor which has been taken in to account is that the surface oxygen content tended to increase by up to 2% At. as a result of the laser processing. This is owed to the thermolytical interaction between the nylon 6,6 material and the CO_2 laser light that gives rise to melting of the nylon surface allowing oxidation to take place. From the results obtained it was found that the apparent surface energy and its components were the most dominating parameter in the modification of wettability which was a result of the mixed state wetting regime owed to the surface topography produced from the different laser-induced patterns.

From the results obtained it was not possible to develop a discernable correlation between the cell response and surface characteristics such as roughness and surface energy. This is due to the fact that a number of factors come in to play which hold the ability to influence how the osteoblast cells

reacted to the nylon 6,6 *in vitro*. It has been seen that for all CO_2 laser surface treated nylon 6,6 samples osteoblast cell response has been improved to become more efficient, allowing cell growth to become quicker. This has been seen through the fact that the cells have covered more area of the nylon 6,6 samples after 24 hours and that the cell density count had increased after 4 days in comparison with the as-received reference control sample. This implies that laser patterned surfaces in this instance gave rise to enhanced biomimetic properties for nylon 6,6 in terms of osteoblast cell response. This response has been observed by instigating cell signaling which has been identified through variations in cell differentiation between each of the samples studied. It has also been observed that all samples incubated over 4 days gave rise to large cover densities of around 100% regardless of laser surface treatment. In terms of morphology the cells were similar to one another when observed using both optical microscopy and SEM after 24 hours incubation, appearing to have more of a bipolar nature. After 4 days the difference in cell morphology became more apparent, with the cell growth showing differing morphologies such as coral-like for the as-received reference control sample and clumped radial growth for the 50 μm and 100 μm hatch patterned samples. This finding can be accounted for by the variation in surface energy and topography instigating cell signaling, which has a major influence on cell morphology. Significantly, it has been seen that over 24 hours and 4 day incubation periods the 50 and 100 μm trench patterns gave rise to improved cell response, having greater cell cover density and mean cell count density in comparison with both the hatch and as-received reference control samples. It was evident from this finding that the trench patterns gave rise to preferential adhesion and cell signaling.

6 – Acknowledgements

7 – References

1. C. Mao, Carbohydr. Polym. 59 (2005) 19.

2. E. Karaca, A. S. Hockenberger, J. Biomed. Mater. Res., Part B. 87B (2008) 580.

3. M. Makropoulou, A. A. Serafetinides, C. D. Skordoulis, Lasers in Medical Science 10 (1995) 201.

4. J. Lawrence, L. Li, Mater. Sci. Eng., A. 303 (2001) 142.

5. L. Hao, J. Lawrence Laser Surface Treatment of Bio-Implant Materials, John Wiley & Sons Inc., New Jersey, USA, 2005.

6. J. Lai, Appl. Surf. Sci. 252 (2006) 3375.

7. P. Roach, D. Eglin, J. Mater. Sci.: Mater. Med. 18 (2007) 1263.

8. M. J. P. Biggs, R. G. Richards, N. Gadegaard, C. D. W. Wilkinson, M. J. Balby, Journal of Orthopaedic Research (2007) 273.

9. A. Diener, B. Nebe, Biomaterials 26 (2005) 383.

10. Z. Ma, Z. Mao, C. Gao, Colloids Surf., B 60 (2007) 137.

11. E. A. Vogler, in: Biomaterials Science, Second edition, Elsevier Academic Press, San Diego, California, USA, 2004. p. 59.

12. C. J. V. Oss, C. F. Gillman, A. W. Neumann, Phagocytic Engulfment and Cell Adhesiveness, Marcel Dekker, New York, USA, 1975.

13. M. S. Kim, K. Gilson, H. B. Lee, Prog. Polym. Sci. in press (2007).

14. M. D. Ball, R. Sherlock, T. Glynn, J. Mater. Sci.: Mater. Med. 15 (2004) 447.

15. K. S. Teh, Y. W. Lu, Topography and wettability control in biocompatible polymer for BioMEMs applications, Proceedings of the 3rd IEEE Int. Conf. on Nano/Micro Engineered and Molecular Systems (6 - 9 January 2008) , Sanya, China (2008) p. 1100.

16. V. Hasirci, H. Kenar, Nanomedicine 1 (2006) 73.

17. R. S. Benson, Nucl. Instrum. Methods Phys. Res., Sect. B. 191 (2002) 752.

18. F. Arefi-Khonsari, Surf. Coat. Technol. 200 (2005) 14.

19. D. Pappas, Surf. Coat. Technol. 201 (2006) 4384.

20. E. M. Harnett, J. Alderman, T. Wood, Colloids Surf. B. 55 (2007) 90.

21. F. Yu, Biomaterials 26 (2005) 2307.

22. H. Mirzadeh, M. Dadsetan, Radiat. Phys. Chem. 67 (2003) 381.

23. M. Dadsetan, H. Mirzadeh, N. Sharifi-Sanjani, M. Daliri, J. Biomed. Mater. Res. 57 (2001) 183.

24. D. G. Rance, in: Surface Analysis and Pretreatment of Plastics and Metals, Applied Science Publishers, Essex, UK, 1982, p. 121.

25. D. G. Waugh, J. Lawrence, Wettability characteristics variation of nylon 6,6 by means of CO_2 laser generated surface patterns, ICALEO 2008 Proceedings (20 - 23 October 2008), 101 (2008) p. 61.

26. Y. C. Jung, B. Bhushan, Nanotechnology 17 (2006) 4970.

27. S. M. Lee, T. H. Kwon, J. Micromech. Microeng. 17 (2007) 687.

28. Y. T. Cheng, D. E. Rodak, Appl. Phys. Lett. 86 (2005) 144101.

29. X. Chen, T. Lu, Sci. China Ser. G-Phys. Mech. Astron. 52 (2009) 233.

30. X. Wu, L. Zheng, D. Wu, Langmuir 21 (2005) 2667.

31. J. Lawrence, L. Li, Laser Modification of the Wettability Characteristics of Engineering Materials, Professional Engineering Publishing Limited, Suffolk, UK, 2001, p. 110.

32. B. Nebe, F. Luthen , R. Lange, P. Becker, U. Beck, J. Rychly, Mater. Sci. Eng., C. 24 (2004) 619.
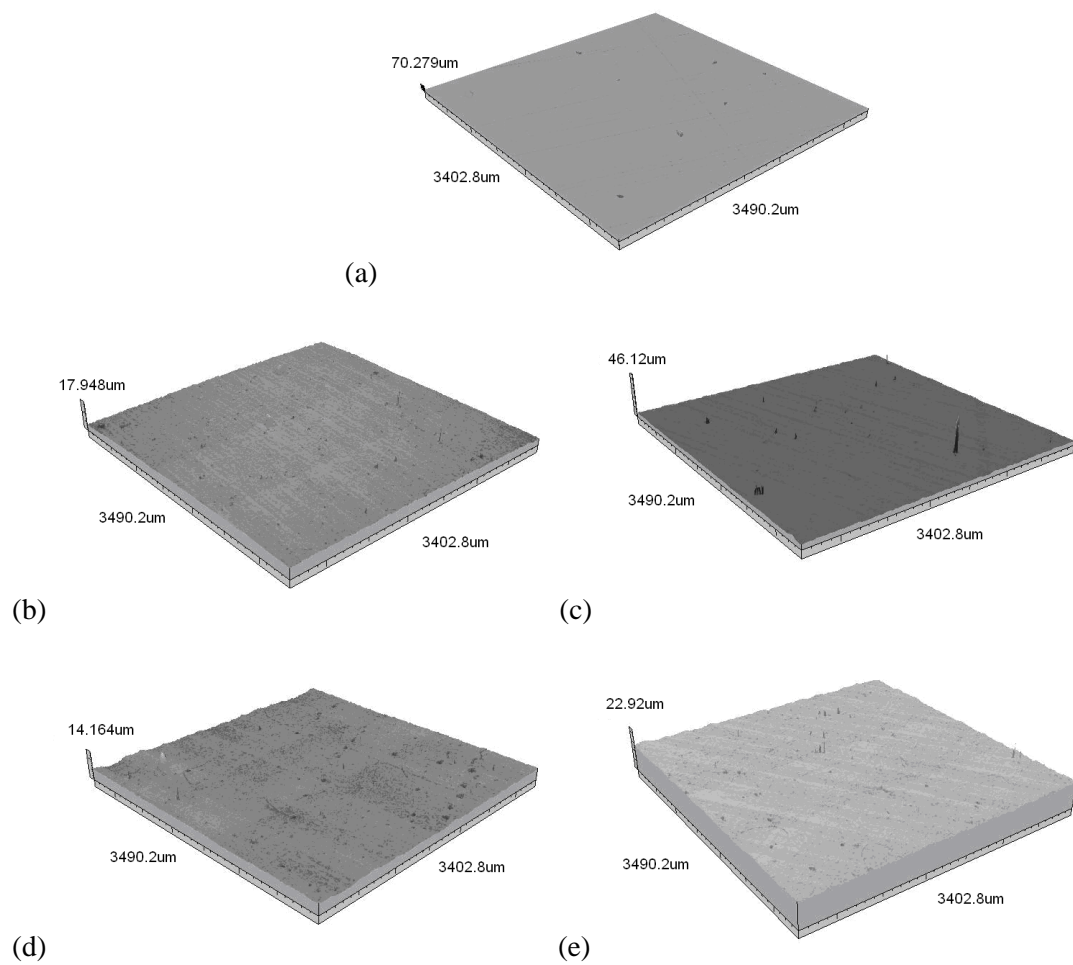
(a)

(b)

(c)

(d)

(e)

Figure 1 – Continuous axonometric images for each of the nylon 6,6 samples – (a) as-received control sample - A1 (b) 50 μm trenches - A3 (c)100 μm trenches - B3 (d) 50 μm hatch - B1 and (e)100 μm hatch - B2.
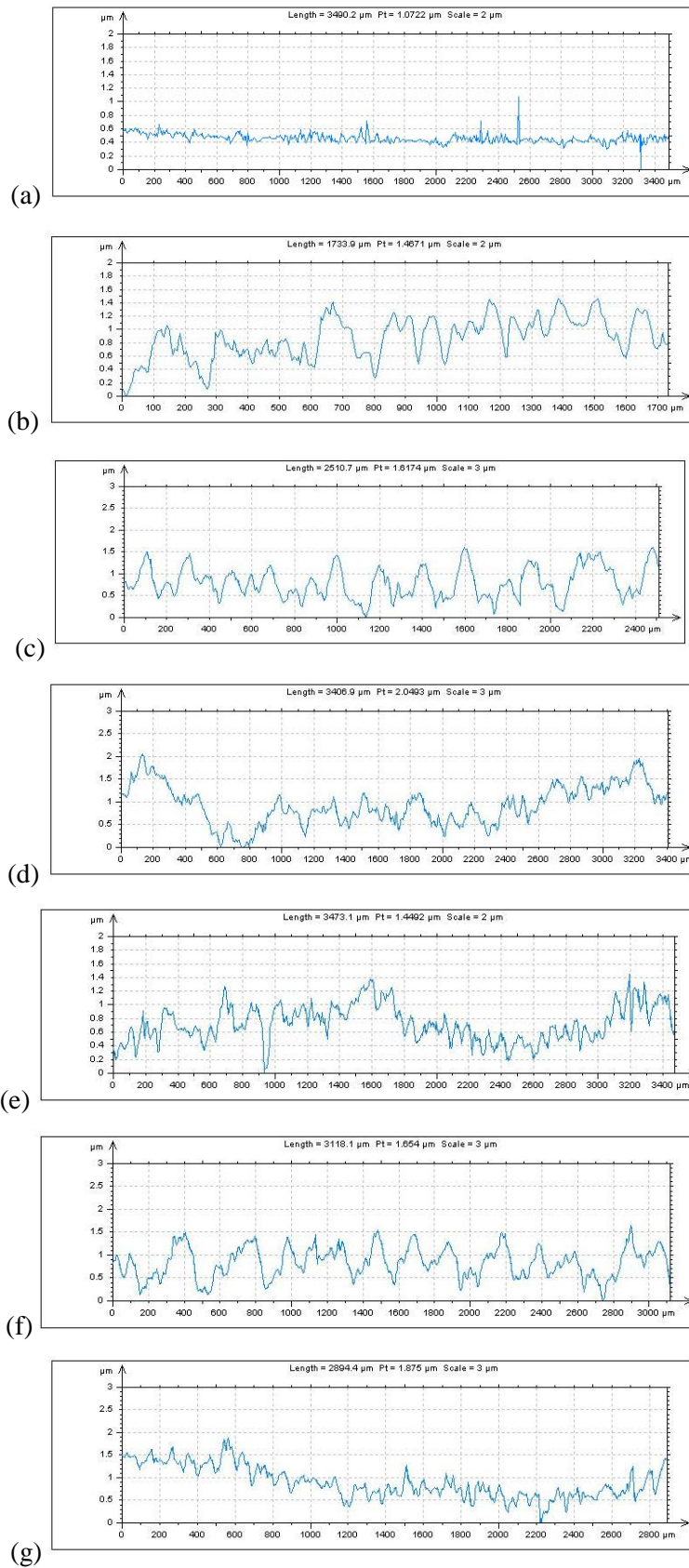
(a)

(b)

(c)

(d)

(e)

(f)

(g)

Figure 2 – Profile extraction for nylon 6,6 samples (a) as-received control sample - A1 (b) 50 µm trenches - A3 (c) 100 µm trenches - B2 (d) 50 µm hatch x-axis - B1 (e) 50 µm hatch y-axis - B1 (f) 100 µm hatch x-axis – B3 and (g) 100 µm trenches y-axis - B3.
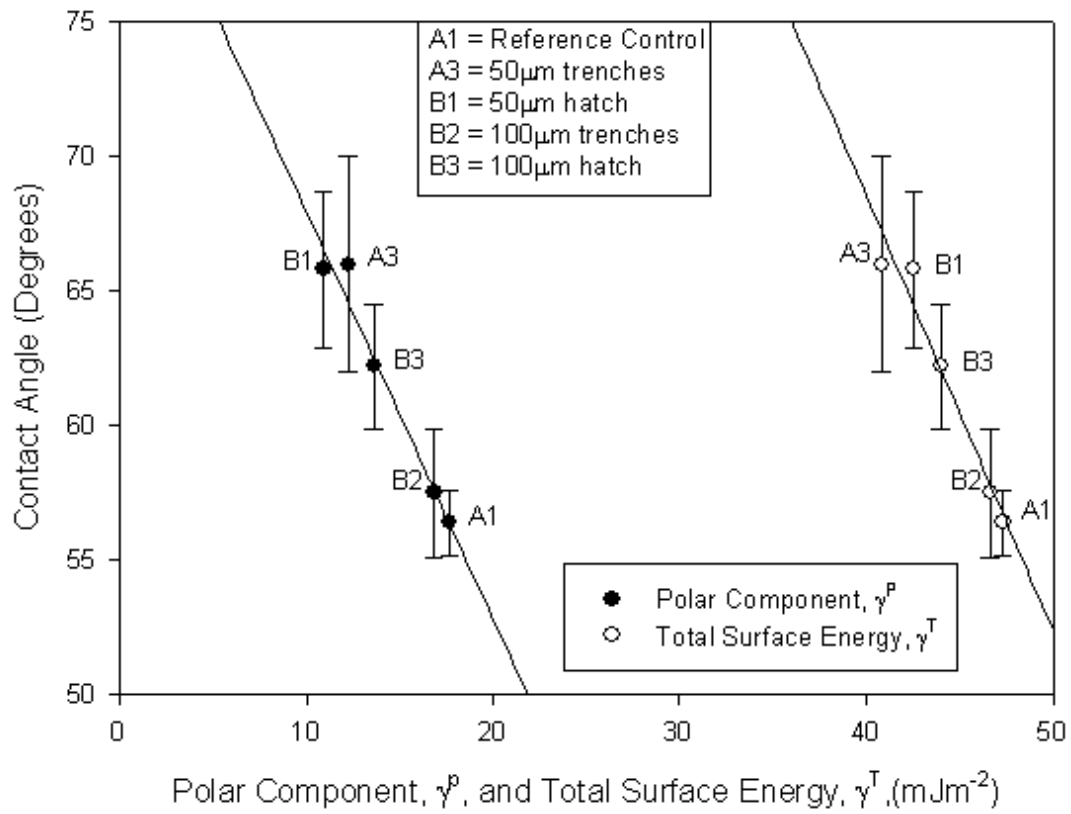
Figure 3 – Characteristic recently advancing contact angle for triply distilled water as a function of polar component, γ^P, and total surface energy, γ^T. (ANOVA showed an overall significance with F = 4.652 and p = 0.004, Scheffe's range test found that there was statistical difference between the 50 μm hatch sample, 50 μm trenches sample and the as-received reference sample, whereas there was no statistical difference between the 100 μm hatch, 100 μm trenches and the as-received control sample*p<0.05)
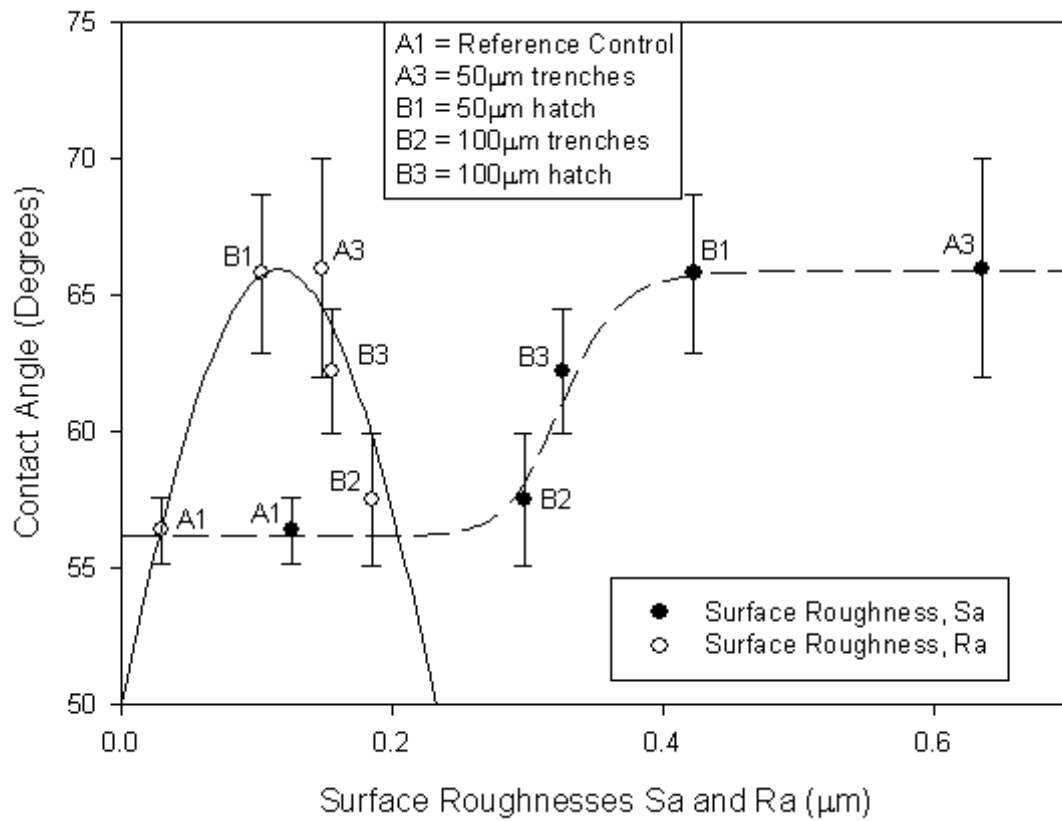
Figure 4 – Characteristic recently advancing contact angle for triply distilled water as a function of the surface roughness parameters Sa and Ra. (ANOVA showed an overall significance with F = 4.652 and p = 0.004, Scheffe's range test found that there was statistical difference between the 50 μm hatch sample, 50 μm trenches sample and the as-received control sample, whereas there was no statistical difference between 100 μm hatch, 100 μm trenches and the as-received control sample*p<0.05)
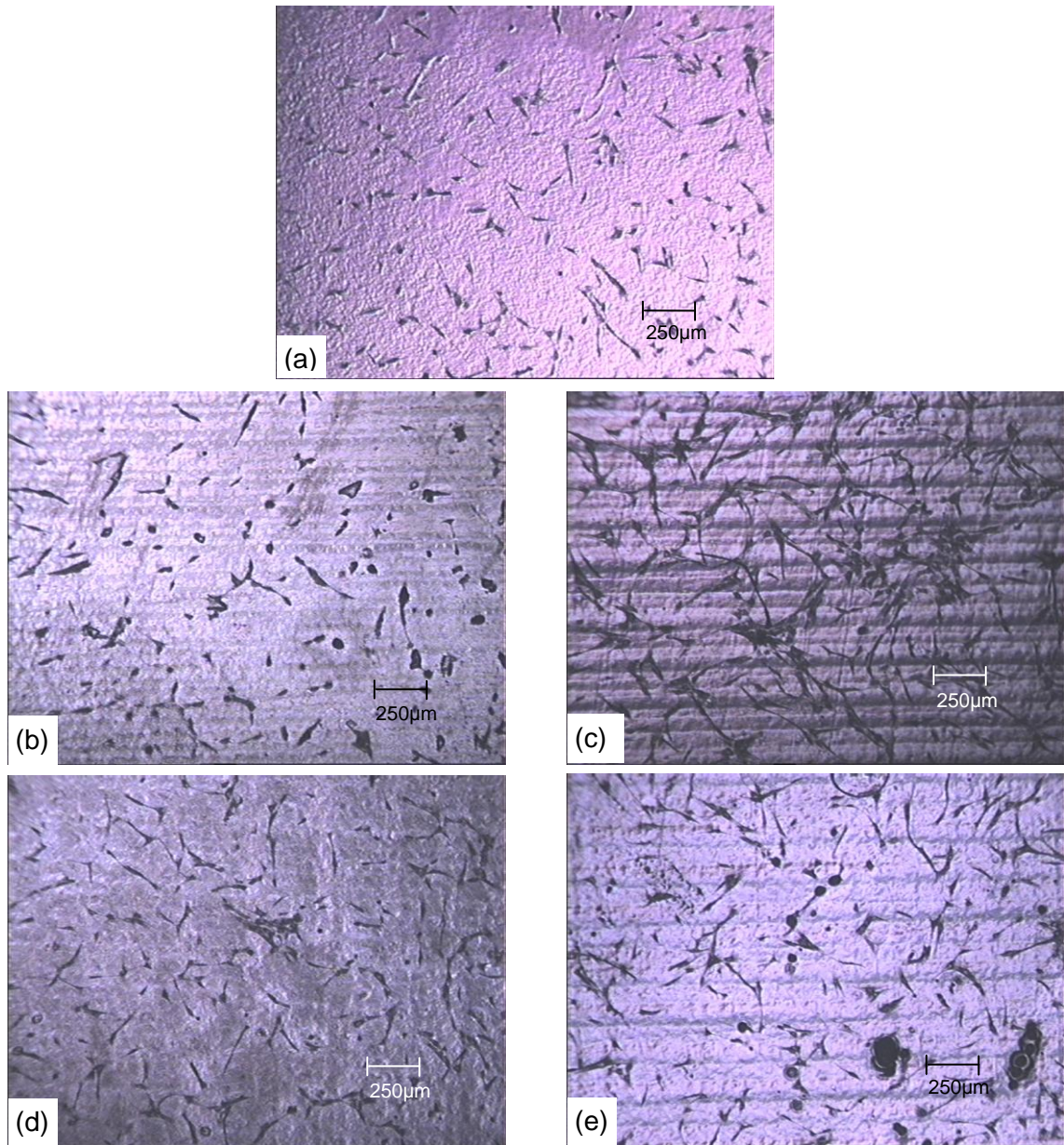
Figure 5 – Optical micrographs of Au coated samples 24 hours post seeding (a) as-received control sample - A1 (b) 50 µm trenches – A3 (c) 100 µm trenches - B3 (d) 50 µm hatch - B1 and (e) 100 µm hatch - B3.
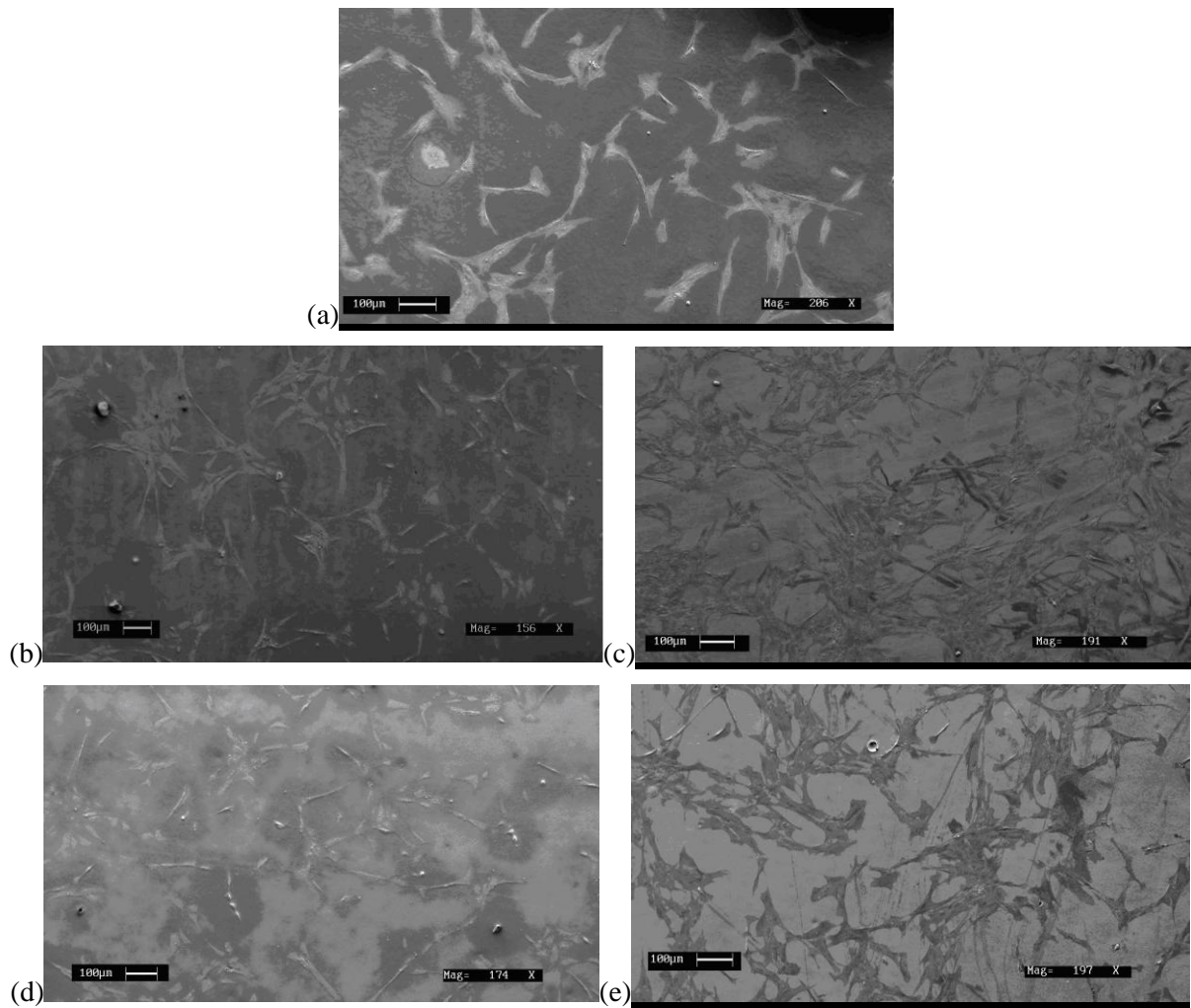
Figure 6 – SEM images of Au coated samples 24 hours post seeding. (a) as-received reference control sample - A1 (b) 50 μm trenches - A3 (c) 100 μm trenches - B2 (d) 50 μm hatch - B1 and (e) 100 μm hatch - B3.
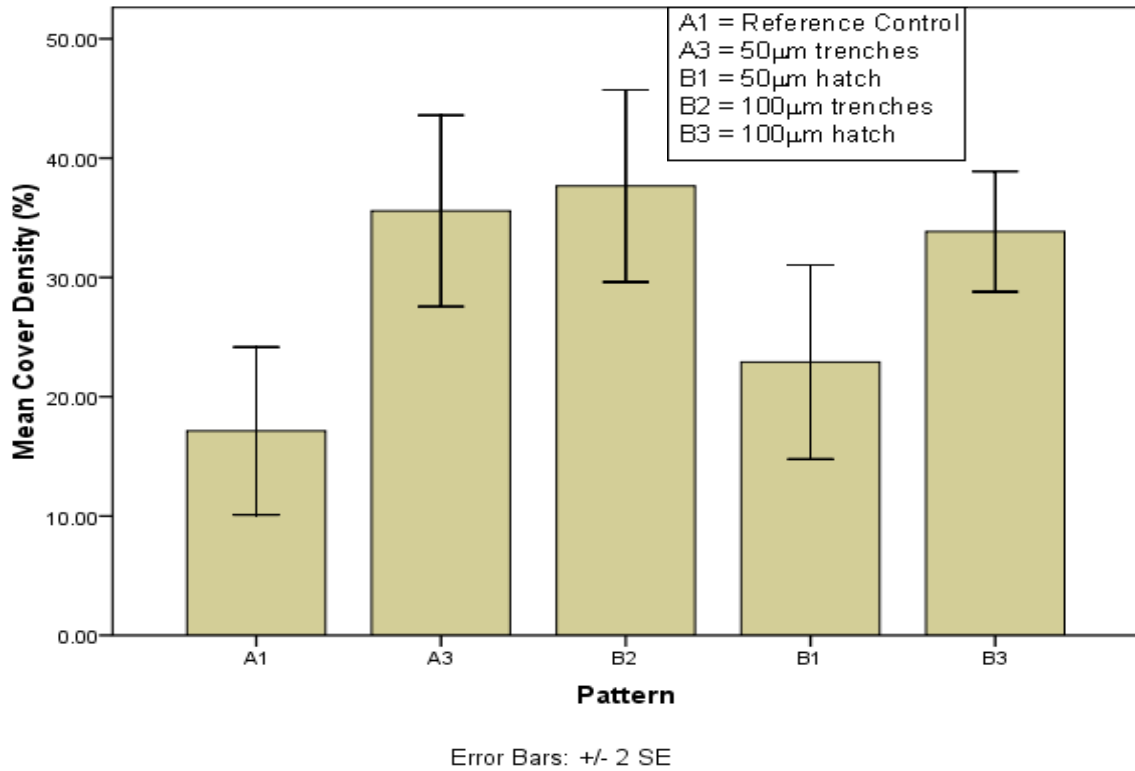
Figure 7 – Histogram showing the cover densities for each of the seeded nylon 6,6 samples after 24 hours. (ANOVA showed an overall significance with F = 6.192 and p = 0.005. Scheffe's range test showed that there was significant statistical difference between samples A2 and B2 and no statistical significance between any of the other samples*p<0.05)
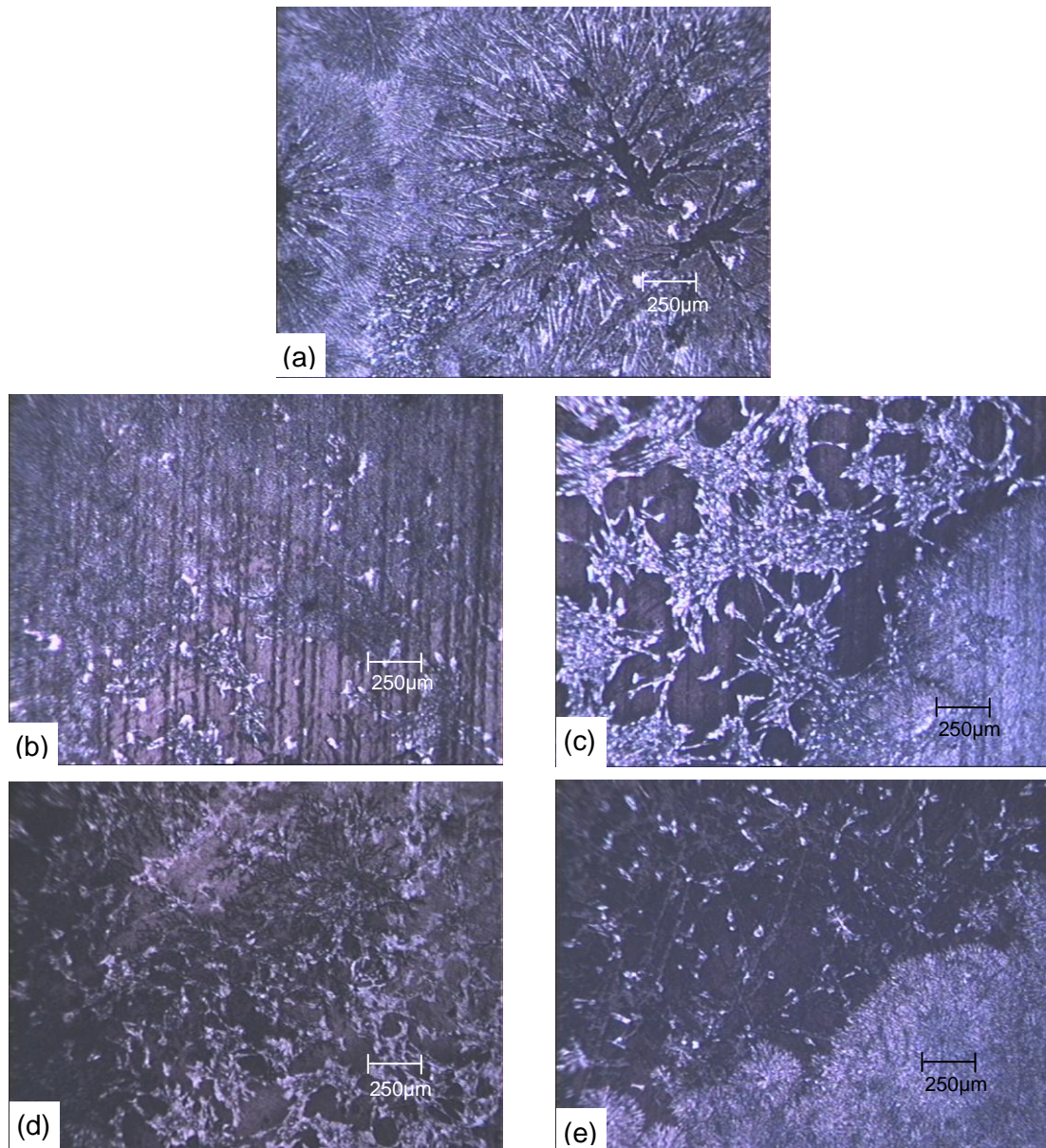
Figure 8 – Optical micrographs of Au coated samples after 4 days incubation (a) as-received control sample - A1(b) 50 μm trench - A3 (c) 100 μm trench - B3 (d) 50 μm hatch - B1 and (e) 100 μm hatch - B3.
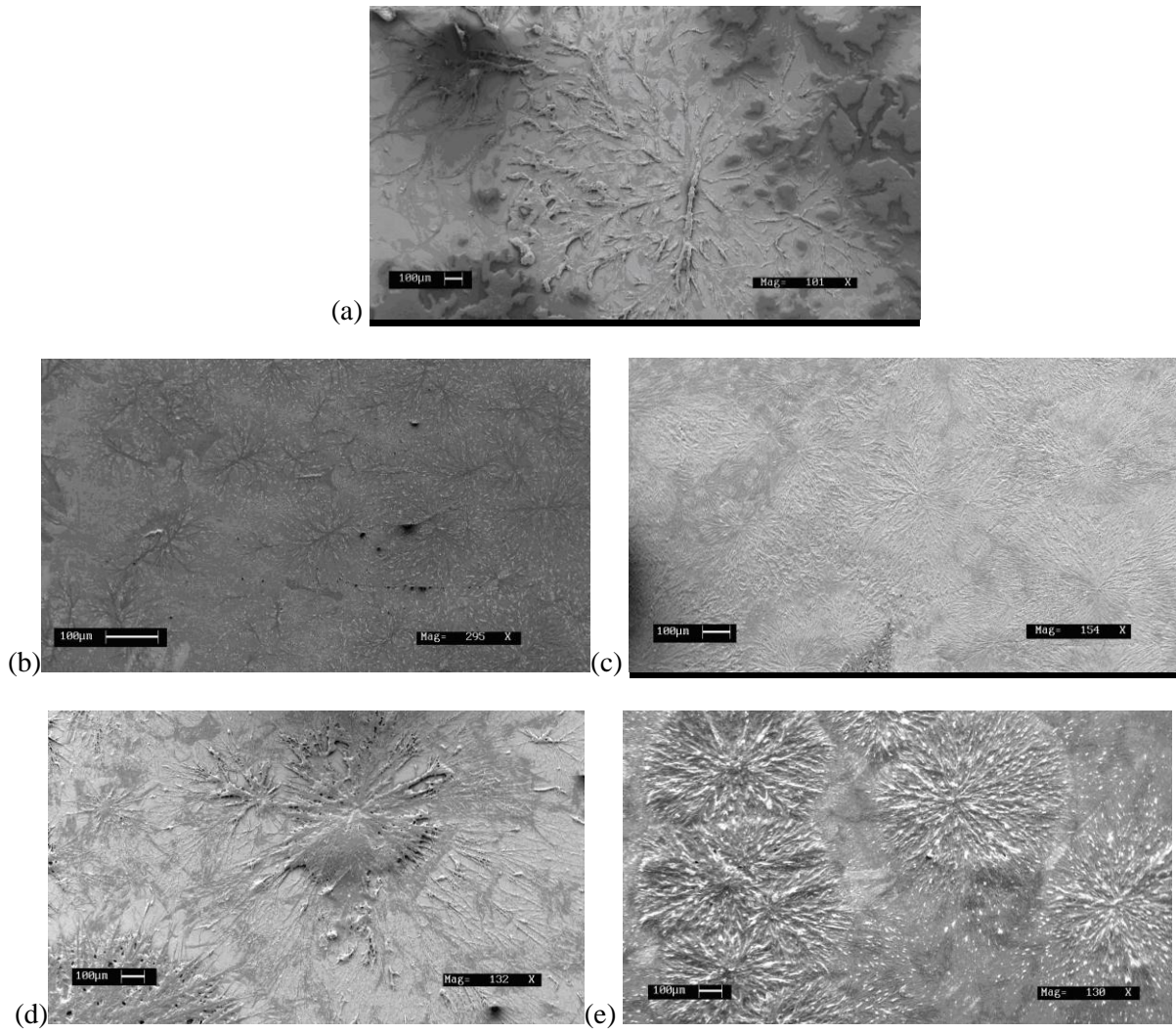
Figure 9 – SEM images of Au coated samples after 4 days incubation (a) as-received control sample - A1 (b) 50 μm trench - A3 (c) 100 μm trench - B2 (d) 50 μm hatch - B1 and (e) 100 μm hatch - B3.
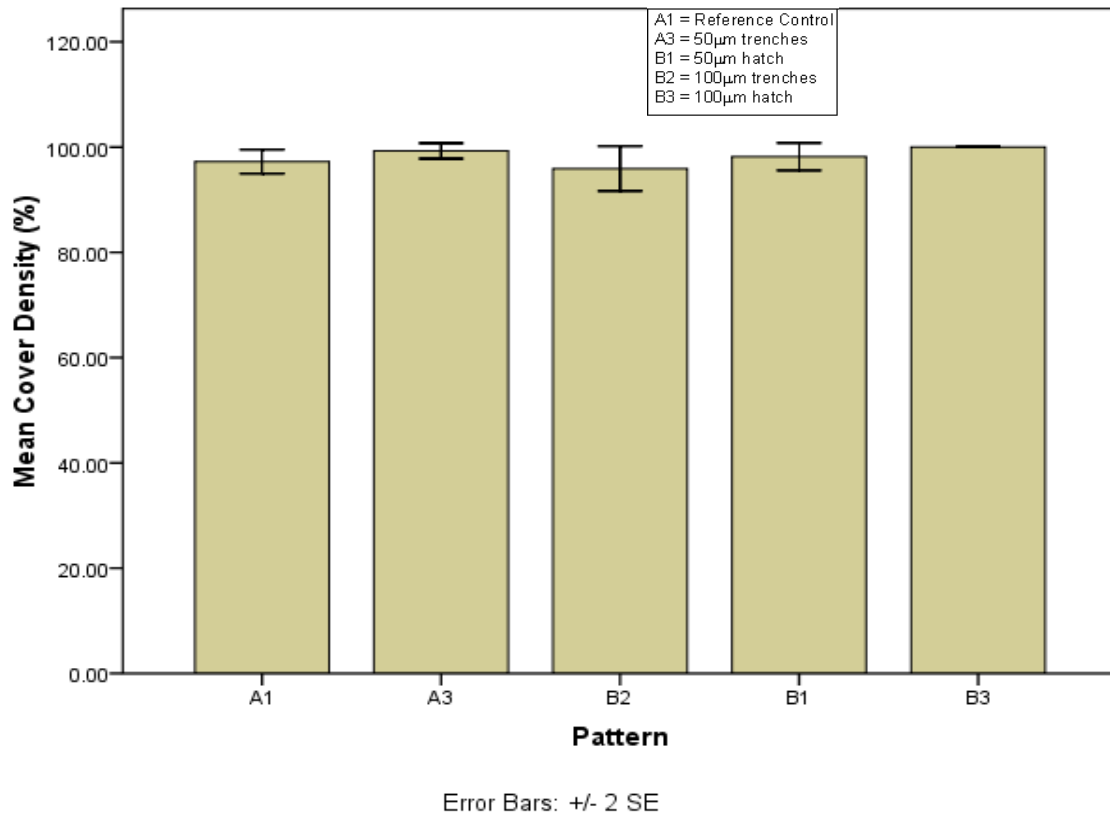
Error Bars: +/- 2 SE

Figure 10 – Cover density for each of the nylon 6,6 samples 4 days after incubation (ANOVA showed that there was not an overall significance with F = 1.892 and p = 0.170. Scheffe's range test showed that there was no statistical difference between any of the samples*p<0.05)
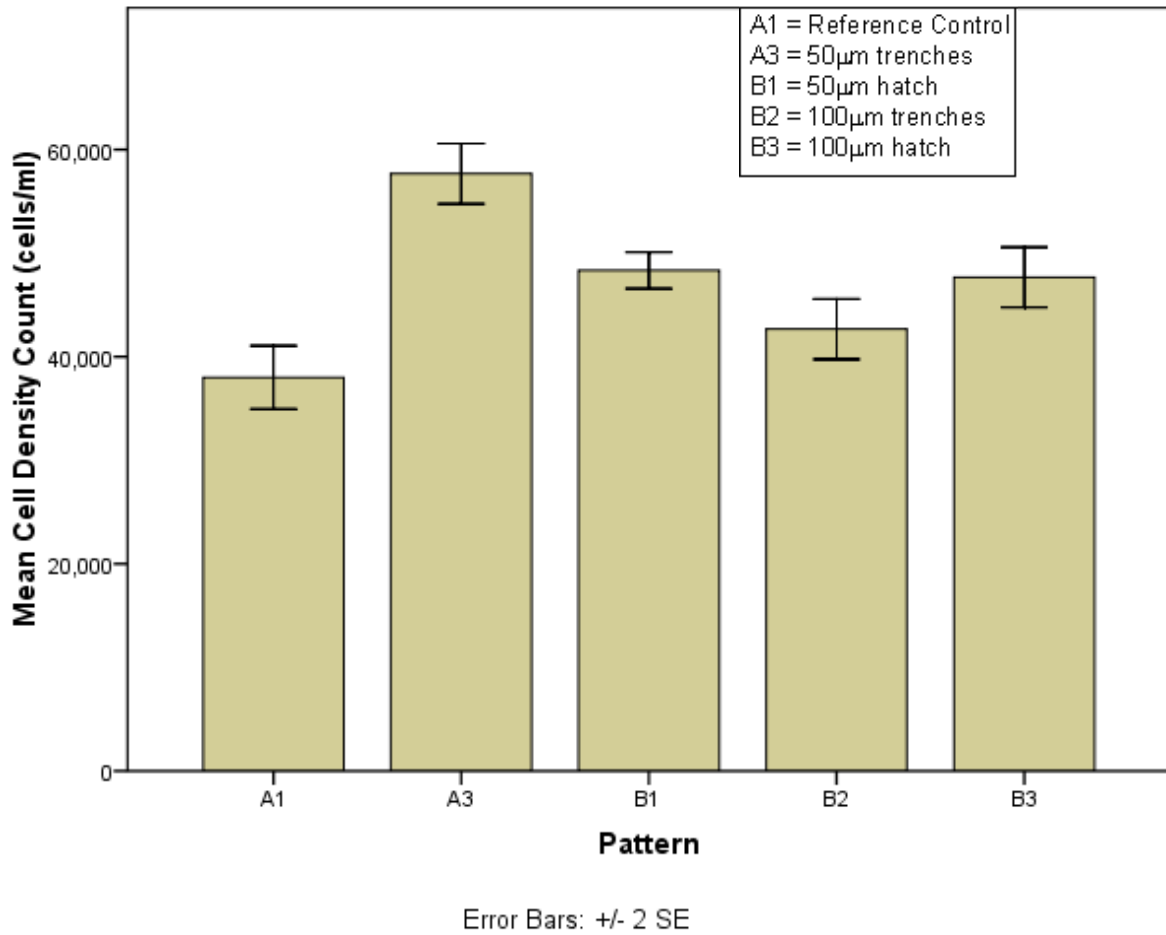
Figure 11 – Cell density count for each of the nylon 6,6 samples 4 days after incubation. (ANOVA showed an overall significance with F = 41.007 and p = 0.000. Scheffe's range test showed that there was statistical significance between all samples apart from A1 and B2; B1 and B2,B3*p<0.5)

Table 1 – Results for the surface roughness, contact angle and surface energy parameters for each sample.

Pattern Shape	Pattern Label	Sa	Ra	Polar Component, γ^P	Dispersive Component, γ^D	Total Surface Energy, γ^T	Contact Angle
		(μm)	(μm)	(mJm^{-2})	(mJm^{-2})	(mJm^{-2})	(°)
As-received reference control sample	A1	0.126	0.029	17.69	29.66	47.34	56.4±1.2
50μm trenches	A3	0.636	0.148	12.24	28.63	40.87	66.0±4.0
100μm trenches	B2	0.297	0.185	16.86	29.83	46.69	57.5±2.4
50μm hatch	B1	0.423	0.103	10.93	31.64	42.58	65.8±2.9
100μm hatch	B3	0.326	0.155	13.63	30.37	44.00	62.2±2.3

Table 2 – Results showing the surface oxygen content for selected samples

Pattern Shape	Surface Oxygen Content (% At.)	Polar Component, γ^P (mJm^{-2})	Contact Angle (°)
As-received reference control sample (A1)	13.26	17.69	56.4±1.2
100µm trenches (B3)	14.05	13.62	57.5±2.4
50µm trenches (B1)	14.33	12.24	66.0±4.0